INSTITUTE FOR SPACE RESEARCH
ACADEMY OF SCIENCES OF THE USSR

Д - 192

V.V.Bezrukikh, T.K.Breus, M.I.Verigin,
P.A.Maysuradze, A.P.Remizov, E.K.Solomatina

DEPENDENCE OF THE EARTH'S MAGNETOPAUSE AND BOW SHOCK POSITIONS ON THE SOLAR WIND PARAMETERS AND THE MAGNETOPAUSE PLASMA STRUCTURE OBSERVED BY CHARGED PARTICLE TRAPS ABOARD THE "PROGNOZ" AND "PROGNOZ-2" SATELLITES

Moscow, 1975

SUMMARY

The investigation of the Earth's magnetopause and bow shock crossings revealed that their variations had correlated with the solar wind pressure ρV^2 variations having the characteristic times of more than 5-10 minuts.

The bow shock velocities corresponding to such variations of the dynamic pressure appeared to be of the order of 10-20 km/sec. The gradual decrease of the total ion flux and spectrum softening registered by the modulation and integral traps, which were identified with a duffuse magnetopause, were observed in 49 events from 93 crossings of the magnetosphere boundary.

The thickness of the diffuse magnetopause was 0,2 R_E + 3 R_E. It increased with the angular distance from the Sun-Earth line.

The sets of ion traps, each includes a modulation trap measuring differential spectrum of ions within the energy range 0 + 3.85 kev and three integral traps were installed on-board the "Prognoz" and "Prognoz-2" satellite for the measurements of ion characteristics in solar wind and the Earth's magnetosphere. Modulation trap and two integral ones were oriented to the Sun, one integral trap - to the anti-solar direction. The measurements of ion fluxes by means of modulation trap were carried out in 8 energy intervals (0-0.03; 0-0.22; 0.22-0.36; 0.36-0.58; 0.62-0.94; 1.0-1.48; 1.58-2.53; 2.8-3.85 kev). The time interval between samplings of energy intervals was about 40.8 sec; hence the total spectrum of ions was taken for 5.44 min. Integral traps registered the sum of flux of ions with energy $E > \max(0, e\varphi_K)$ where φ_K is a satellite potential and electron flux with energy > 70 ev; they were sampled once every 40.8 sec. The detailed description of equipment and sensors is given in [1] .

In this paper the results of the measurements by means of modulation traps in the region of shock wave and magnetopause from the "Prognoz" and "Prognoz-2" satellites in April - October, 1972 (from 29 June to 17 September the results of simultaneous measurements) are analyzed. The data of integral ion traps are used only for refining the moments of crossing of the magnetopause and the shock wave front since these data were obtained with the greater time resolution than those from modulation traps.

1. Study of the shock wave front and magnetopause position variations

The simultaneous measurements in solar wind and the magnetosphere with two or more vehicles are the interesting and still relatively rare possibility for study of the correlation of the different processes. Therefore for the study of the shock front and magnetopause variations precisely the data of the simultaneous measurements from the "Prognoz" and "Prognoz-2" were used.

The crossings of the front and magnetopause by these satellites were identified by the typical change of shapes of spectra registered with modulation traps and the variation of current measured with integral traps. In the magnetosheath modulation traps recorded the broadening of ion spectra in comparison with those in solar wind and the shifting of spectral maximum to lower energies. Thermalization (and, consequently, flux increase) of electrons and the ion bulk velocity decrease result in that in the magnetosheath currents of integral traps turn out to be negative. Near the magnetopause the level of currents taken by both modulation and integral traps sharply decreased and was close to the sensitivity threshold of traps [2].

The crossings of the shock frond and magnetopause observed from one of the satellites were compared with the changes of these boundaries calculated from the data on the solar wind dynamic pressure obtained by the other satellites; the results of comparison are shown in Fig. 1-3.

It follows from the gas-dynamical calculations [3] that under the sufficiently great Mach numbers the distances up to the shock front R_s and magnetopause R_M (if an angular distance φ of a current point from the direction to the Sun is not too large) can be approximately written as

$$R_{S,M} = C_{S,M} (\rho V^2)^{-1/6} f_{S,M}(\varphi), \qquad (1)$$

where $C_{S,M}$ =const, ρ -is a density and V - is a solar wind velocity, $f_{S,M}(\varphi)$-is a function that decribes the shape of front and magnetopause. It is seen from Eq.(1) that with φ =const the change of the distance up to the boundary depends only on the variation of dynamic pressure of solar wind ρV^2

To exclude the relative change of the positions of the boundaries and the satellites connected with φ -angle variation occuring during the orbital motion of the satellites the orbits were reduced to the same value of angle in each time interval analyzed. For this form fs,m(φ) was used for the average shock front and magnetopause calculated over all the crossings registered (Fig.4). The similar transformation of a trajectory had been taken by Binsack and Vasyliunas [4] who first obtained the confirmation of the dependence of the front position on the solar wind dynamic pressure based on the data obtained from the three satellites.

Fig.4 shows the positions of the "Prognoz" and "Prognoz-2" satellites at the moments of their crossings of the shock front (Fig.4a) and magnetopause (Fig.4b) in coordinates $X, \sqrt{Y^2+Z^2}$ (X-axis passes through the Earth center and is directed to the Sun): points refer to single crossings of the boundaries, dashed lines - to multiple crossings, solid lines in Fig.4b show the smooth transfer from the magnetosheath to the magnetosphere (see §2). The boundaries were approximated by the second-order curves symmetrical relative to X-axis. The r.m.s. distances along normal to the boundary of crossings presented in Fig.4 were minimized over the three parameters.

Table 1 gives the parameters characterizing the average position of the front and magnetopause calculated under the above-mentioned approximation.

Table I

Boundary type	ε	Standoff distance $R_{s,m}$ (R_E)	p (R_E)	X_F focus position (R_E)
front	0.85	13.1	23.4	0.5
magnetopause		9.9	10.1	4.5

It should be noted that the average position of the front was also calculated in [5] based on the data from electrostatic analyzers on the "Prognoz" satellites. The difference between the average front parameters obtained in [5] (hyperbola with ε = 1.09, p =28.6 R_E R_s = 13.7 R_E) and those obtained in the present paper can be associated both with the use in [5] a less number of experimental points and with the fact that the r.m.s. radial deviations of these points from the symmetrical second-order curve with focus at the Earth center was minimized in [5] .

In Fig.1-3 blackened parts of the orbits correspond to time of passes of satellites through the magnetosheath S and the magnetosphere M; thin and unblackened parts - to the satellite locations in solar wind W and in the magnetosheath S. In all Figures the trajectories of the satellites were reduced to some fixed angles φ (see above); a scale for distances (along Y-axis) is logarithmic one that allows to fit the calculated plot - $\frac{1}{6}$ lg (ρV^2) (stepped line in Figures) with the observed crossings of the front and magnetopause by means of this plot shifting along the Y-axis. This procedure gives the possibility to get rid of the use of the inaccurate empirical coefficient $C_{s,m}$ in Eq.(1) and constant multiplier in calculations of ρV^2 based on spectra measured. It should be noted that in the solar wind dynamic pressure calculations energetic intervals with the maximum readings make the most contribution (one-two intervals for a spectrum). Thus calculated ρV^2 values represent practically the mean ones for the time period $\leqslant$ 1 - 1.5 min.

The calculated positions of the front and magnetopause in Fig,1, 2a and 3a are determined using the solar wind dynamic pressure values ρV^2 averaged over 2-3 spectra, i.e. 5-10 min taking into account of all the mentioned-above and in Fig. 2b and 3b - over the ρV^2 values for each spectrum ($\sim$ 1 - 1.5 min).

It is seen from Figs. 1, 2a and 3a that there is a rather close agreement between the positions of the boundaries calculated and observed. The comparison of these Figures with Figs. 2a and 3b shows that the agreement essentially deteriorates for the non-averaged data. Hence we can conclude that the characteristic time for the establishment of the quasi-stationary positions of both the shock wave front and magnetopause connected to the solar wind pressure variations is equal to about 5-10 min. Note that this time on the order of magnitude is in agreement with time of propagation of fast magnetoacoustic waves ($\sim 70 \div 100$ km/sec) transmitting the information from the shock front to magnetopause and back (at distance $\Delta \sim 3 \div 5\ R_E$).

The statistic study of the dependence of the front and magnetopause positions on solar wind dynamic pressure with the use of a great deal of the data obtained from the IMP-4 satellite was carried out by Fairfield [6]. He concluded that from the solar wind dynamic pressure the magnetopause position could be predicted worse than the front position. It was evidently associated with the large interval of time between the moments of crossing magnetopause by the satellite and the period of its location in undisturbed solar wind for which dynamic pressure was determined.

The simultaneous measurements from the two satellites widely separated in space are conveniently used for the direct estimation of the shock front motion velocity. Fig.5 (the same symbols as in Figs.1-3) shows the case when the "Prognoz" and "Prognoz-2" satellites flying to meet each other at the orbital sections being in the subsolar region of the near-earth space registered the multiple crossings of the shock front. At 14^h 11^m UT the "Prognoz" crossed the shock front and entered the magnetosheath. At this time the "Prognoz-2" being in solar wind began to record the monotonous fall of ρU^2 i.e. the shock front should continuously remove from the Earth (without back-forward motions, see Fig.5b). Really, at 14^h22^mUT the front reached the "Prognoz-2" that was also removing from the Earth. So for 10 min the shock front passed about 2 R_E along normal to its average surface and its average velocity was consequently equal to $\sim$20 km/sec.

In the other case analyzed in the similar way (31/7/72) the front motion velocity amounted to $\sim$10 km/sec. These estimations on the order of magnetude agree with the experimental estimations for the front movement mean velocity equal to about 10-20 km/sec previously obtained by Holzer et al. [7], Heppner et al. [8], Kaufmann et al. [9] and with the theoretical calculations by Völk and Auer [10] and Auer [11].

In paper by Formisano et al. [12] where the front motion velocity was calculated with using Rankin-Hugoniot relations the average value of velocity equal to $\sim$85 km/sec was obtained. Such estimations are connected with the significant difficulties in determining concentration and a vector of the ion bulk velocity in the magnetosheath for which it is difficult to find the suitable form of the distribution function (e.g., see [13]).

We can evidently agree with the authors of [10] that the high velocities of the bow shock motion obtained in some papers [12, 14] can be associated with the extremal conditions in solar wind (extraordinary small values of Mach numbers, tangential discontinuities with concentration jumps > 4 or < 1/3, shock waves ets.) that are realized rather rarely.

2. Study of the magnetopause plasma structure

The analyzis of magnetopause crossings by the "Prognoz" and "Prognoz-2" satellites showed that in 49 among 93 cases under consideration the gradual change of character of spectra occured that lasted from 10 min to several hours (in some cases). Magnetopause corresponding to such crossings will be further called as diffuse one like in [15] and [16] , for example.

Fig.6a gives the example of the characteristic variations of primary ion spectra and currents from integral traps oriented to the Sun for the crossing of the sharp magnetopause on 28/5/72 and Fig.6b - for the crossing of the diffuse magnetopause on 9/9/72. In the first case the sharp changes of character of spectra from modulation trap and current from integral trap occured for time less than 40.8 sec. Fig.6c illustrating the crossing of diffuse magnetopause on 16/5/72 by the "Prognoz" satellite shows the changes of ion flux $nv=3.67\cdot10^{17}\sum_i I_i$ (where I_i is a current in amperes registered in i-th energy interval) and a number of spectra corresponding to the time moments marked in nv-curve by arrows; φ-angles (Sun-Earth-satellite) and Kp-indexes concerned with the period of the magnetopause crossing by the satellites are also given in this Figure. As it is seen from Figs. 6b and c when transferring from the magnetosheath to the magnetosphere the gradual change (decrease) of ion flux and the gradual softening of spectra (relative diminution of currents in the energy intervals corresponding to the higher energies) occur at distance of about 2 R_E. The maximum gradient of ion flux was observed at distance of 1 R_E.

The results of measurements of ion spectra by means of five similar modulation traps installed aboard the "Prognoz-3" satellite in 1973 (Fig.7) can serve as the evidence for the fact that the observed softening of spectra is not the result of plasma flux deflection from the trap when the satellite is moving to the magnetosphere. The axis of four traps composed 30°-angle with the axis of the central trap oriented to the Sun; ion spectrum within the energy range 0 ÷ 4 kev was taken for 10 min in 6 energy intervals.

When ion flux deflected of the central trap by α-angle the modulation is observed of currents in lateral traps because of the satellite rotation around the axis of the central trap; and with $\alpha > 15°$ the maximum flux will get into one of lateral traps. Fig.7 presents currents in all the five traps: the top curve shows currents in the central trap; the bottom curve does the direction of the energy increase in each spectrum. It is seen from this Figure that when crossing the diffuse magnetopause within all the energy intervals fluxes in the central trap exceed the maximum flux in the other traps, i.e. the deflection of the ion flux direction from the axis of the central trap oriented to the Sun composes $\alpha < 15°$.

Fig.8 gives the data of the simultaneous measurements of the absolute value $|B|$, polar angle θ and azimuth angle φ of the magnetic field vector, ion spectra and ion flux nv from the "Prognoz" satellite on 8/5/72 during crossing the diffuse magnetopause. The data of the magnetic measurements were kindly presented by Sh.Sh.Dolginov and E.G.Eroshenko. It is seen from Fig.8 that with the smooth change of ion spectra and ion flux at distance of about 0.5 R_E

during crossing the diffuse magnetopause all the characteristics of the magnetic field do not also reveal sharp jumps.

From Fig. 4b, where parts of solid lines show the position of the satellite during crossing the diffuse magnetopause, it can be seen that diffuse magnetopause is frequently observed at the sufficiently small angles φ and its thickness on an average increases with φ growth.

Table II shows the ratios of the number of the diffuse magnetopause registrations to the total number of magnetopause crossing within the given intervals of solar-ecliptic latitudes.

Table II

φ^{o}_{SE}	diffuse	sharp	in all	%
0 - 30	24	23	47	51%
30-50	8	14	22	36%
50 - 70	17	7	24	71%

It is clear from Table II that the diffuse boundary was most frequently observed in the latitudinal belts of 50-70° and 0-30°. However it should be considered with caution to the tendency of the latitudinal distribution of diffuse magnetopause outlined in Table II due to the relative small number of the data available.

The comparison of the diffuse boundary observations with the data of the simultaneous measurements of the interplanetary magnetic field from HEOS-2 [17] shows that at the presence of the north component B_N of the interplanetary magnetic field the diffuse magnetopause average thickness was about 0.8 R_E and at the south component B_S presence it increased up to $\sim 2\ R_E$.

Reviewing the published data we can conclude that the opinion on magnetopause as a sharp boundary discontinuity at least in the subsolar region is prevaling at present with thickness of the order of Larmor radius for ions ~100 km (see, e.g. [7,8,16,18,19]etc). The diffuse boundary was observed in the magnetosphere tail with "Pioneer-8" (at distances of about 30 ÷ 40 R_E) [15], "Explorer-35" (near the lunar orbit ~60 R_E) [20] as well as from the "Vela" satellites (at distances ~18 R_E) [21,22]. The absence of the sharp boundary (diffuse magneto-pause) is mentioned from analysis of the magnetic data obtained on occasional orbits of IMP-I satellite [23,24], OGO-I (near the equatorial plane at the down and dusk sectors of the magne-tosphere) [8], the plasma and magnetic data from some crossings of magnetopause by IMP-2 satellite [16] in the subsolar region of the magnetosphere.

In laboratory experiments [25] the plasma inflow into polar clefts (as well as into the polar cusps in spacecraft experi-ments [26,27]) and into equatorial cleft was observed. The latter begins at the dayside of the artificial magnetosphere approxi-mately at 14^hLT and continues up to the magnetosphere tail.

Finally the interaction of the magnetosheath plasma with the magnetosphere which can lead to the broadening of the sharp magnetopause is discussed in some theoretical works(viscous-type interaction [28], reconnection of the interplanetary magnetic field having a south component with the earth dipole field [29], the development at the boundary of the various plasma instabilities, e.g. [24,30]).

As it can be concluded from the characteristics of the diffuse magnetopause considered at the present paper, that have been observed from the "Prognoz" and "Prognoz-2" as well as from the "Prognoz-3" satellite, it resembles a boundary layer found in the magnetosphere tail by Hones et al. [21,22] from the "Vela" satellites.

The diffuse boundary latitudinal distribution has the tendency similar to the observational data presented in [26], [27, 8] as well as to the data of laboratory experiments [25]. that evidenced for the possible plasma inflow into polar and equatorial clefts and for the magnetopause instability at these latitudes. This similarity as well as some dependence of the diffuse magnetopause thickness registered from "Prognoz" and "Prognoz-2" on the presence of the interplanetary magnetic field south component can be discussed in connection with the origin of the diffuse magnetopause and require the further investigatior

REFERENCES

I. V.V.Bezrukikh, A.P.Belyashin, G.I.Volkov, K.I.Gringauz, L.I.Denshikova, G.N.Zastenker, V.G.Kaptsov, V.F.Kopylov, V.S.Mokrov, L.S.Musatov, Yu.N.Pozdnov, A.P.Remizov, M.Z.Khokhlov. Study of the plasma in the Earth's magnetosphere and the interplanetary space with the satellites of "Prognoz" serie, Geomagn. i aeron., I4, N 3, 400, I974.

2. K.I.Gringauz, G.N.Zastenker, M.Z.Khokhlov. Variations of the magnetopause position from "Prognoz" and "Prognoz-2" charged particle trap data. Kosmitcheskie issled., I2, N 6, I974.

3. J.R.Spreiter, A.L.Summers, A.Y.Alksne, Hydromagnetic flow around the magnetosphere, Planet.Space Sci., I4, 223, I966.

4. J.H.Binsack, V.M.Vasyliunas, Simultaneous IMP-2 and OGO-I observations of bow shock compression, J.Geoph.Res., 73, 429, I968.

5. O.L.Vaisberg, A.A.Zertsalov, V.V.Temny, Ye.E.Berezin. Bow shock and α-component in the magnetosheath according to the measurements from the high-latitude satellite "Prognoz", Kosmitcheskie issled., I2, N I, 80, I974.

6. D.H.Fairfield. Average and unusual locations of the Earth's magnetopause and bow shock. J.Geoph.Res., 76, 6700, I97I.

7. R.E.Holzer, M.G.McLeod, E.J.Smith. Preliminary results from the OGO-I search coil magnetometer: Boundary positions and magnetic noise spectra. J.Geoph.Res., 7, I48, I966.

8. J.P.Heppner, M.Sugiura, T.L.Skillman, B.G.Ledley, M.Campbell. OGO-A magnetic field observations, J.Geoph.Res., 72, 54I7, I967.

9. R.L.Kaufmann. Shock observations with the Explorer-I2 mangetometer. J.Geoph.Res., 72, 2323, I967.

I0. H.J.Volk, R.D.Auer. Motions of the bow shock induced by interplanetary disturbances, J.Geoph.Res., 79, 40, I974.

II. R.D.Auer. Magnetohydrodynamic aspects of the Earth's bow shock. 2. Motion induced by directional discontinuities, J.Geoph.Res., 79, 34, 5I22, I974.

I2. V.Formisano, P.C.Hedgecock, G.Moreno, F.Palmiotto, J.K.Chao, Solar wind interaction with Earth's magnetic field; 2. Magnetohydrodynamic bow shock. J.Geoph.Res., 78, 373I, I973.

I3. V.Formisano, G.Moreno, F.Palmiotto, P.C.Hedgecock. Solar wind interaction with the Earth's magnetic field; I.Magnetosheath, J.Geoph.Res., 78, I9, 37I4, I973.

I4. E.W.Grinstadt, P.C.Hedgecock, C.T.Russell. Large scale coherence and high velocities of the Earth's bow shock on February I2, I969, J.Geoph.Res., 77, III6, I972.

I5. D.S.Intrilligator, J.H.Wolf, Evidence of a diffuse magnetopause boundary, J.Geoph.Res., 77, 5480, I972.

I6. D.H.Fairfield, N.F.Ness. Magnetic field measurements with the IMP-2 satellite, J.Geoph.Res., 72, 2379, I967.

I7. P.C.Hedgecock. Heos interplanetary field measurements: Bartels solar rotation plots of 3-hourly average, December I968-December I972. Preprint, Imperial College physics department, London, S.W.7. October, I973.

I8. L.J.Cahill,Jr., V.L.Patel. The boundary of the geomagnetic field, August to November I96I. Plan.Space Sci., I5, 997, I967.

I9. M.P.Aurby, M.G.Kivelson, C.T.Russell. Motion and structure of the magnetopause, J.Geoph.Res., 76, 673, I97I.

20. H.C.Howe, G.L.Siscoe. Magnetopause motions at Lunar distance determined from the Explorer-35 plasma experiment, J.Geoph.Res., 77, 607I, I972.

2I. E.W.Hones,Jr, J.R.Asbridge, S.J.Bame, M.D.Montgomery, S.Singer, S.I.Akasofu. Measurements of magnetotail plasma flow made with Vela-4B, J.Geoph.Res., 77, 5503, I972.

22. S.I.Akasofu, E.W.Hones,Jr, S.J.Bame, J.R.Asbridge, A.T.Lui, Magnetotail and boundary layer plasmas at a geocentric distance of I8 R_E: Vela-5 and 6 observations, J.Geoph.Res., 78, 7257, I973.

23. N.F.Ness, C.S.Scearce, J.B.Seak. Initial results of the IMP-I magnetic field experiment, J.Geoph.Res., 69, 353I, I964.

24. B.R.Boller, H.L.Stolov. Explorer-I8 study of the stability of the magnetopause using a Kelvin-Helmholtz instability criterion, J.Geoph.Res., 78, 8078, I973.

25. E.M.Dubinin, I.M.Podgorny. Particle precipitation and radiation belt in laboratory experiments, J.Geoph.Res., 79, I926, I974.

26. L.A.Frank, Plasma in the Earth's polar magnetosphere. J.Geoph.Res., 76, 5202, I97I.

27. C.T.Russell, C.R.Chappel, M.D.Montgomery, M.Neugebauer, F.L.Scarf, OGO-5 observations of the polar cusp on November I, I968, J.Geoph.Res., 76, 6743, I97I.

28. W.I.Axford. Viscous interaction between the solar wind and the Earth's magnetosphere, Plan.Space Sci., I2, 45. I964.

29. J.W.Dungey. The interplanetary magnetic field and the auroral zones, Phys.Rev.Letters, 6, 47, 1961.

30. D.J.Sothwood, The hydromagnetic stability of the magnetospheric boundary, Plan.Space Sci., 16, 587, 1968.

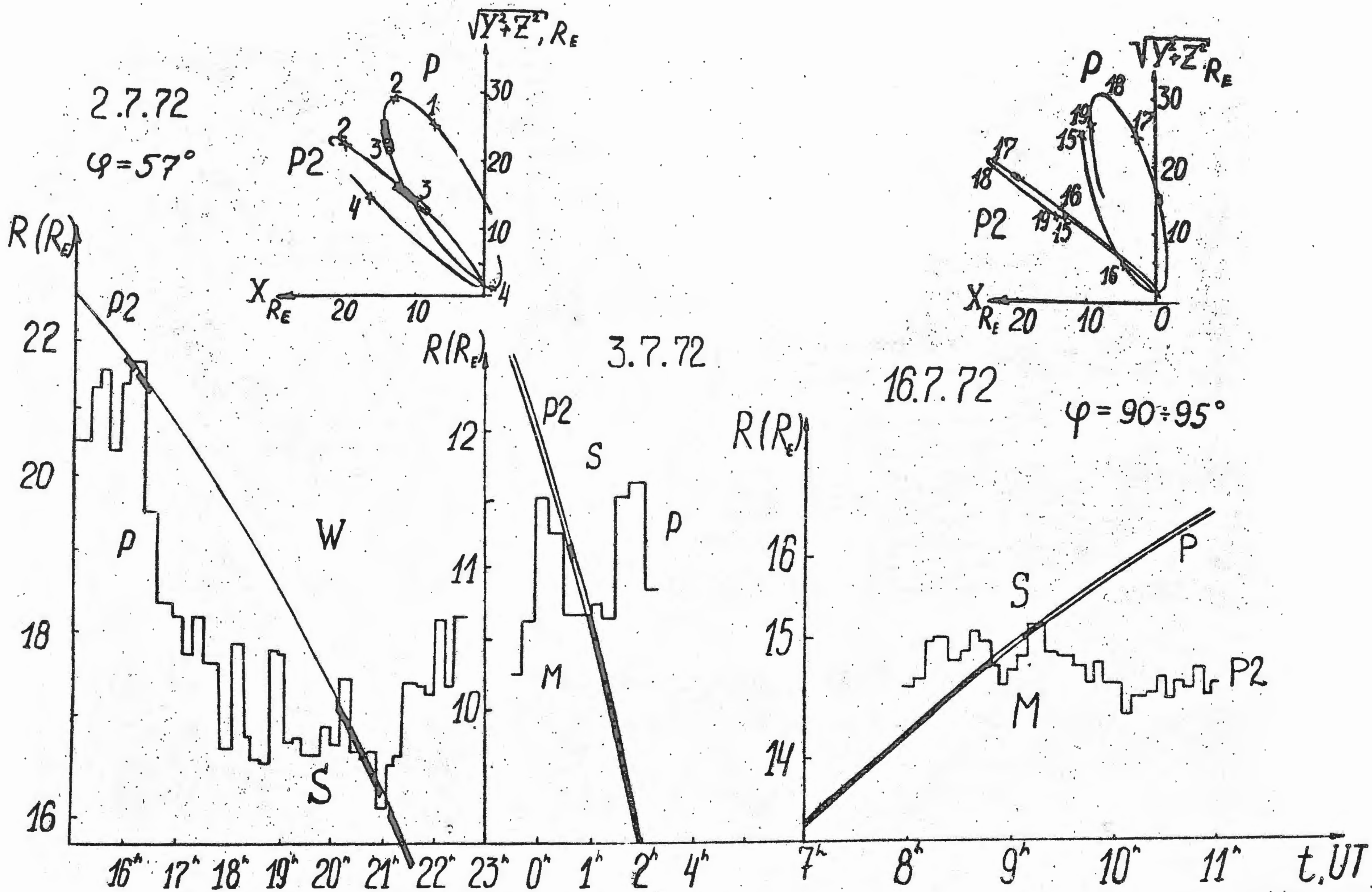

Fig.1.

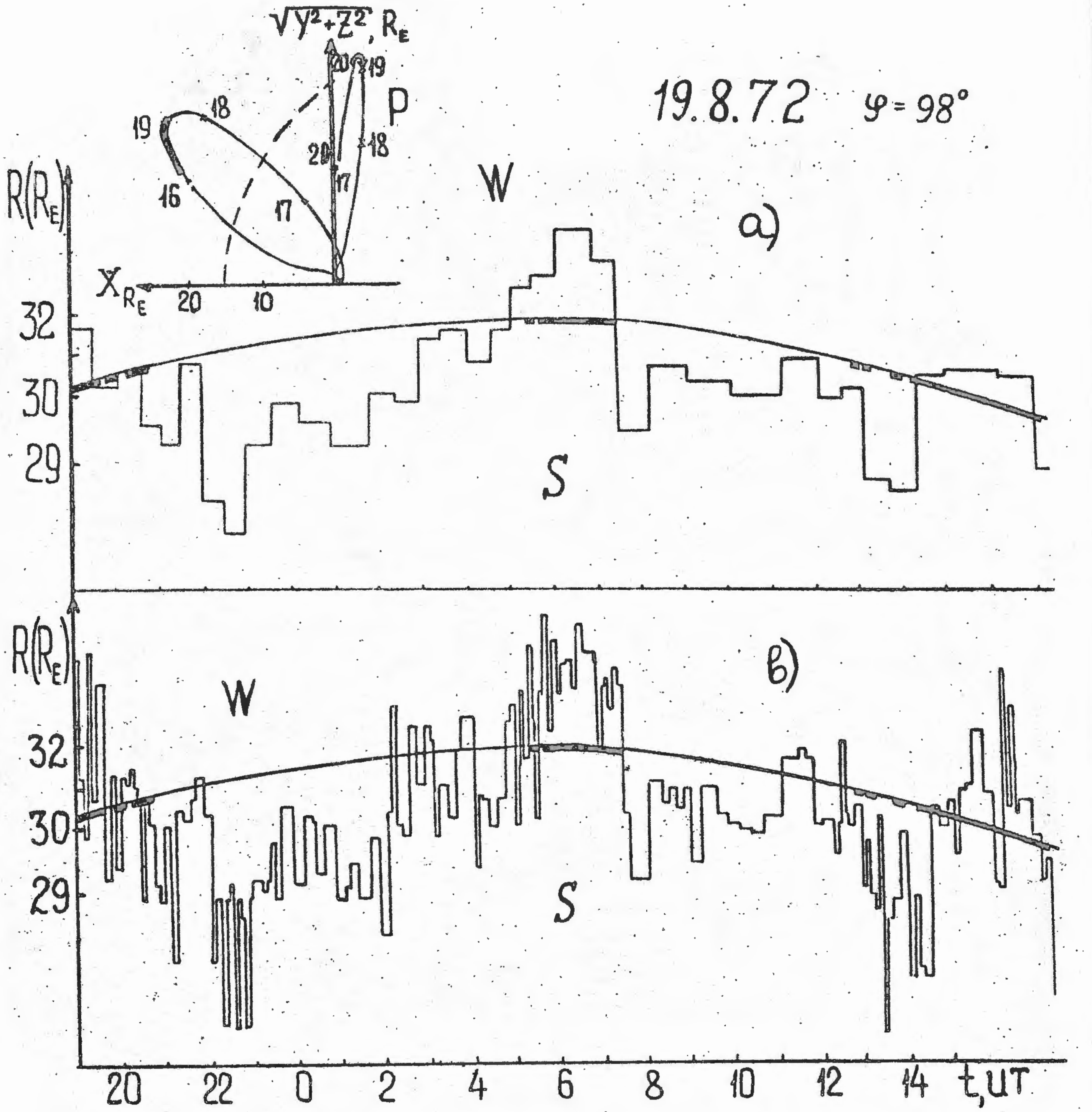

$\sqrt{Y^2+Z^2}$, R_E
19.8.72
φ = 98°
W
a)
R(R_E)
X_{R_E}
20
10
32
30
29
S
P
б)
t, UT
20
22
0
2
4
6
8
10
12
14

Fig.2

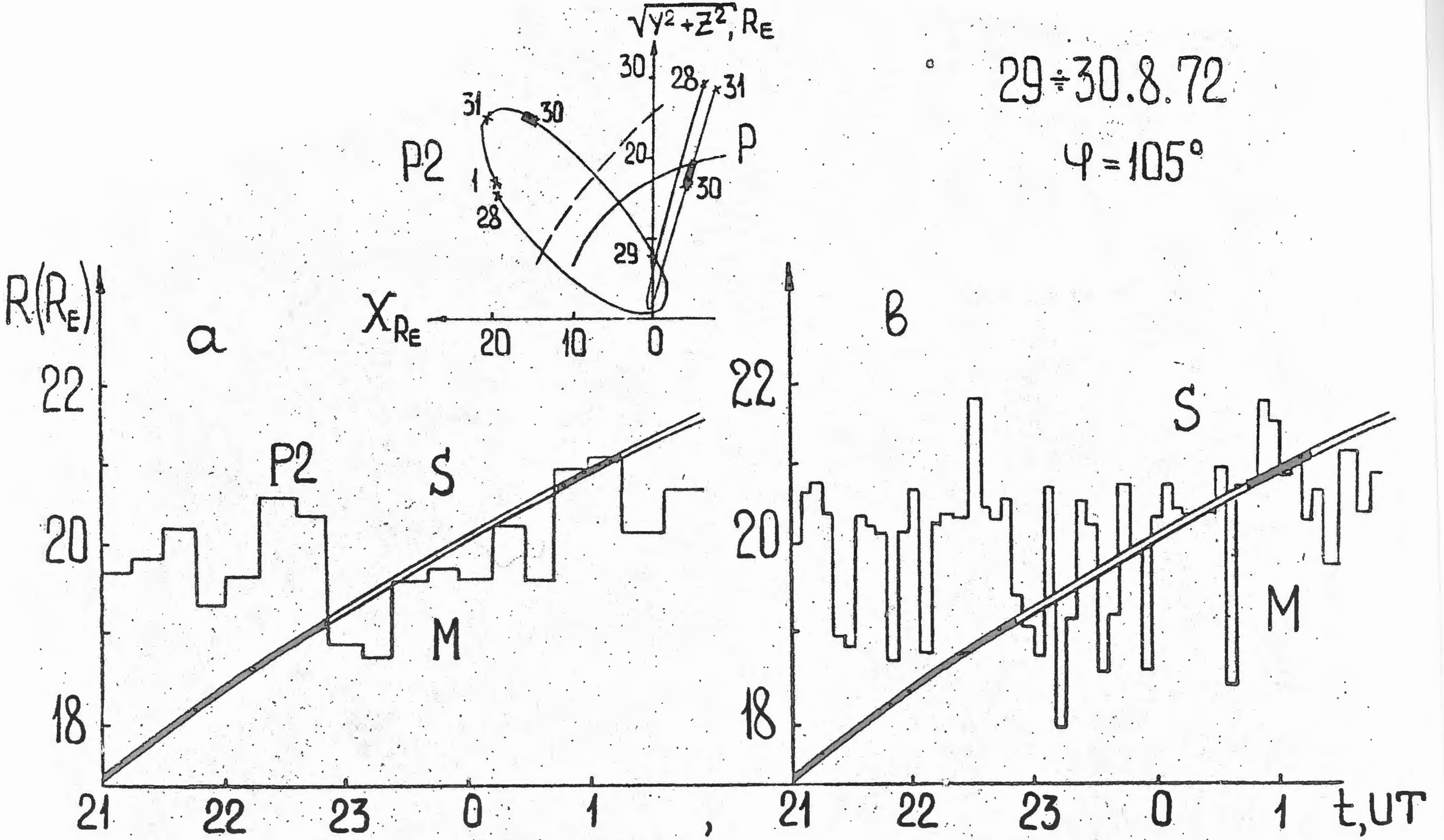

$\sqrt{Y^2+Z^2}$, R_E
30
28
31
30
P2
1
28
20
P
30
29
X_{R_E}
20
10
0
29÷30.8.72
φ = 105°
R (R_E)
a
22
20
18
P2
S
M
21
22
23
0
1
B
22
20
18
S
M
21
22
23
0
1
t, UT

Fig. 3

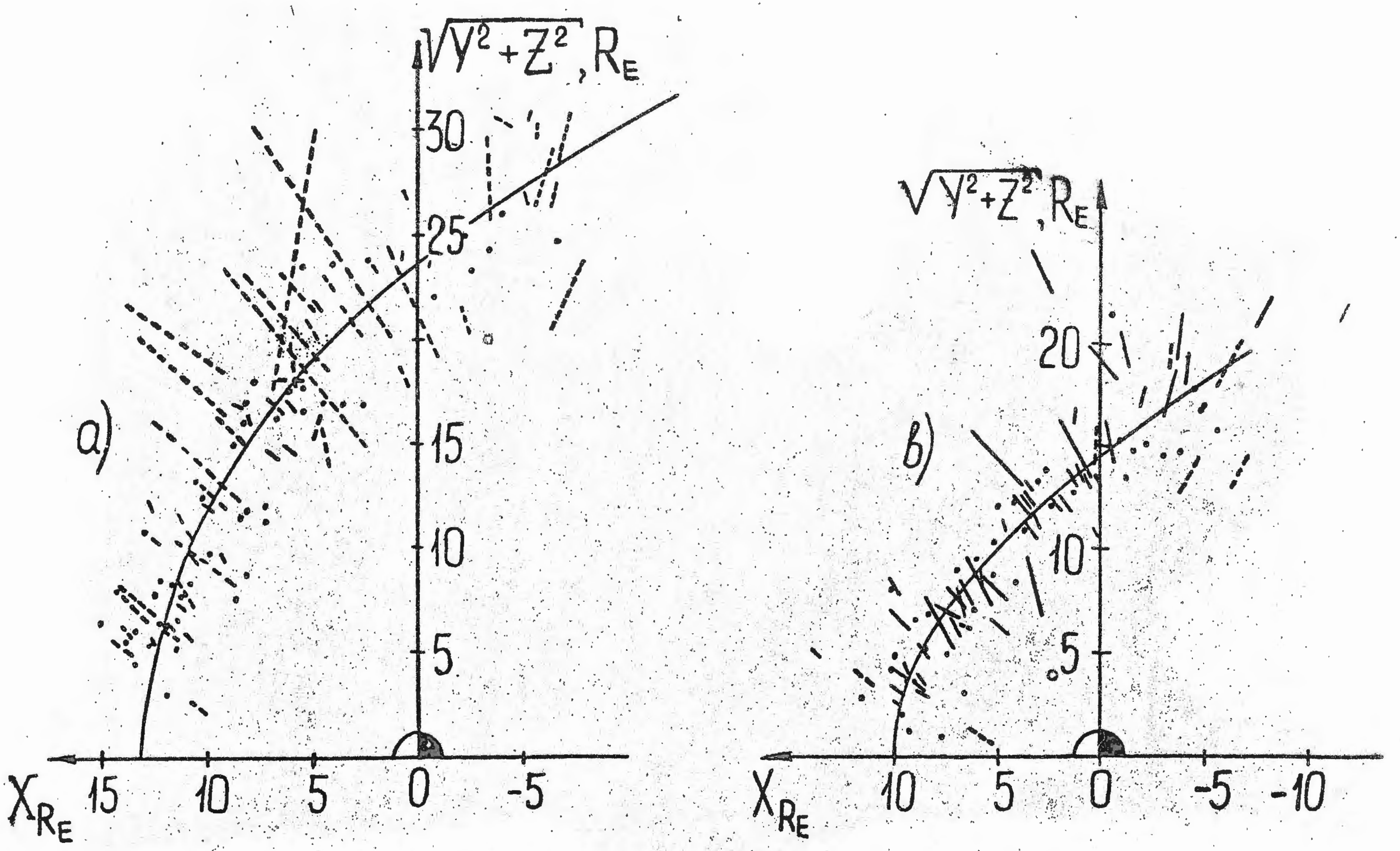

$\sqrt{Y^2+Z^2}, R_E$
30
25
15
10
5
a)
X_{R_E}
15
10
5
0
-5
$\sqrt{Y^2+Z^2}, R_E$
20
10
5
б)
X_{R_E}
10
5
0
-5
-10

Fig. 4

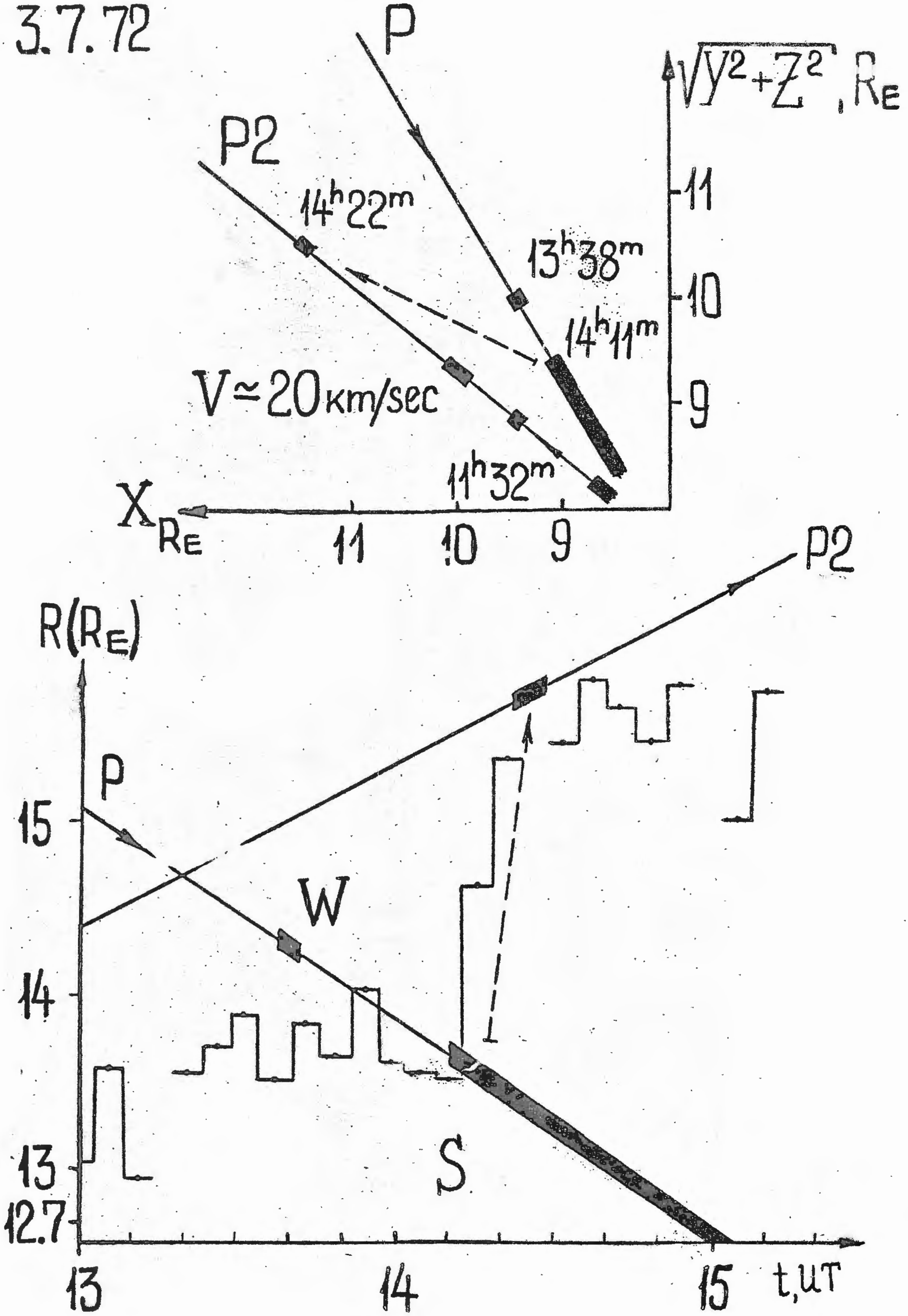
3.7.72
P
P2
$\sqrt{Y^2+Z^2}$, R_E
11
10
9
14^h22^m
13^h38^m
14^h11^m
V≃20km/sec
11^h32^m
X_{R_E}
11
10
9
P2
R(R_E)
P
15
W
14
13
12.7
S
13
14
15
t,UT

Fig. 5

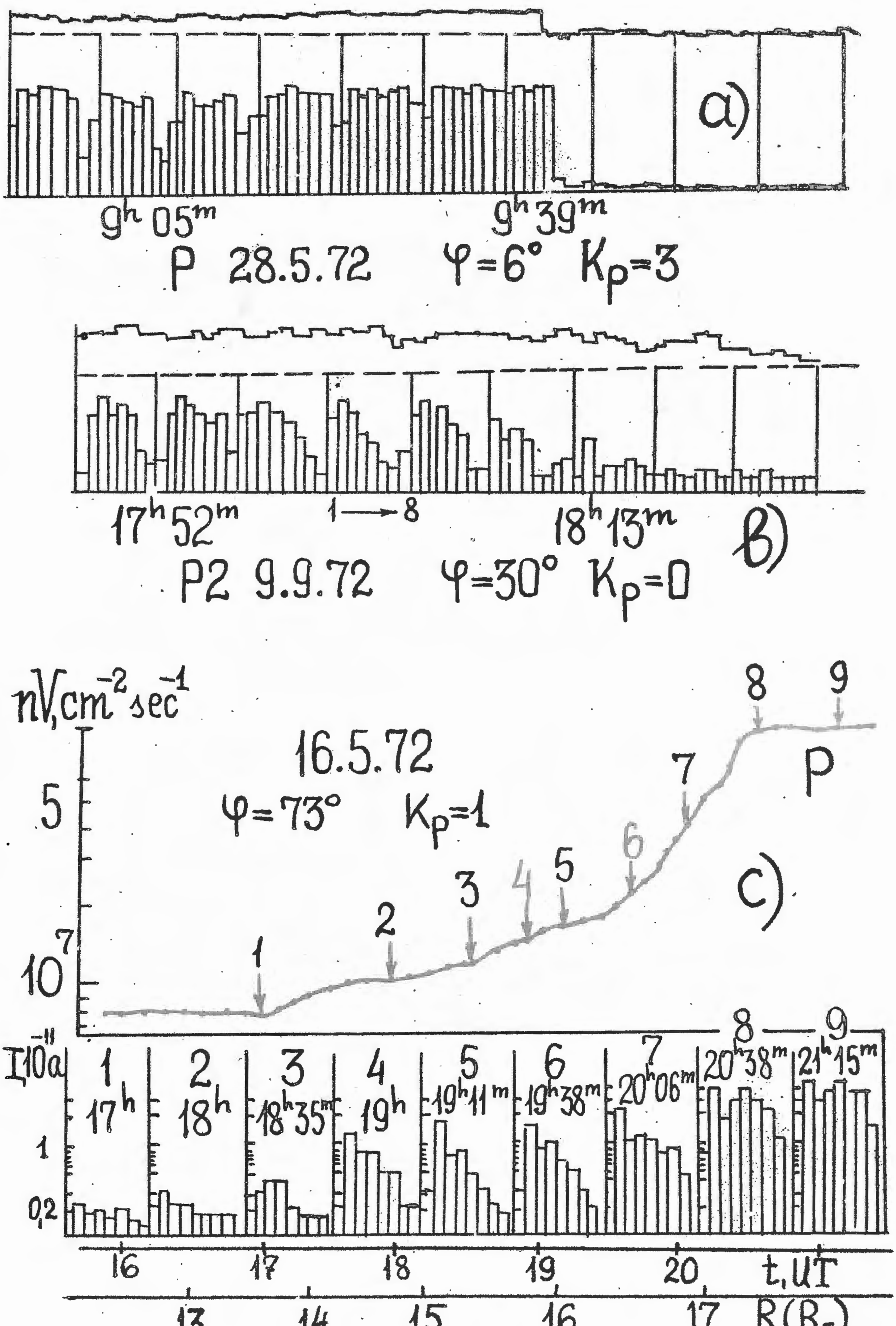

a)
9h 05m
9h 39m
P 28.5.72 φ=6° Kp=3
17h 52m
1 → 8
18h 13m
в)
P2 9.9.72 φ=30° Kp=0
nV, cm-2 sec-1
16.5.72
φ=73° Kp=1
P
c)
5
10^7
1 2 3 4 5 6 7 8 9
I 10^-11 a
1
0,2
17h
18h
18h 35m
19h
19h 11m
19h 38m
20h 06m
20h 38m
21h 15m
16 17 18 19 20 t, UT
13 14 15 16 17 R(R_E)

Fig.6

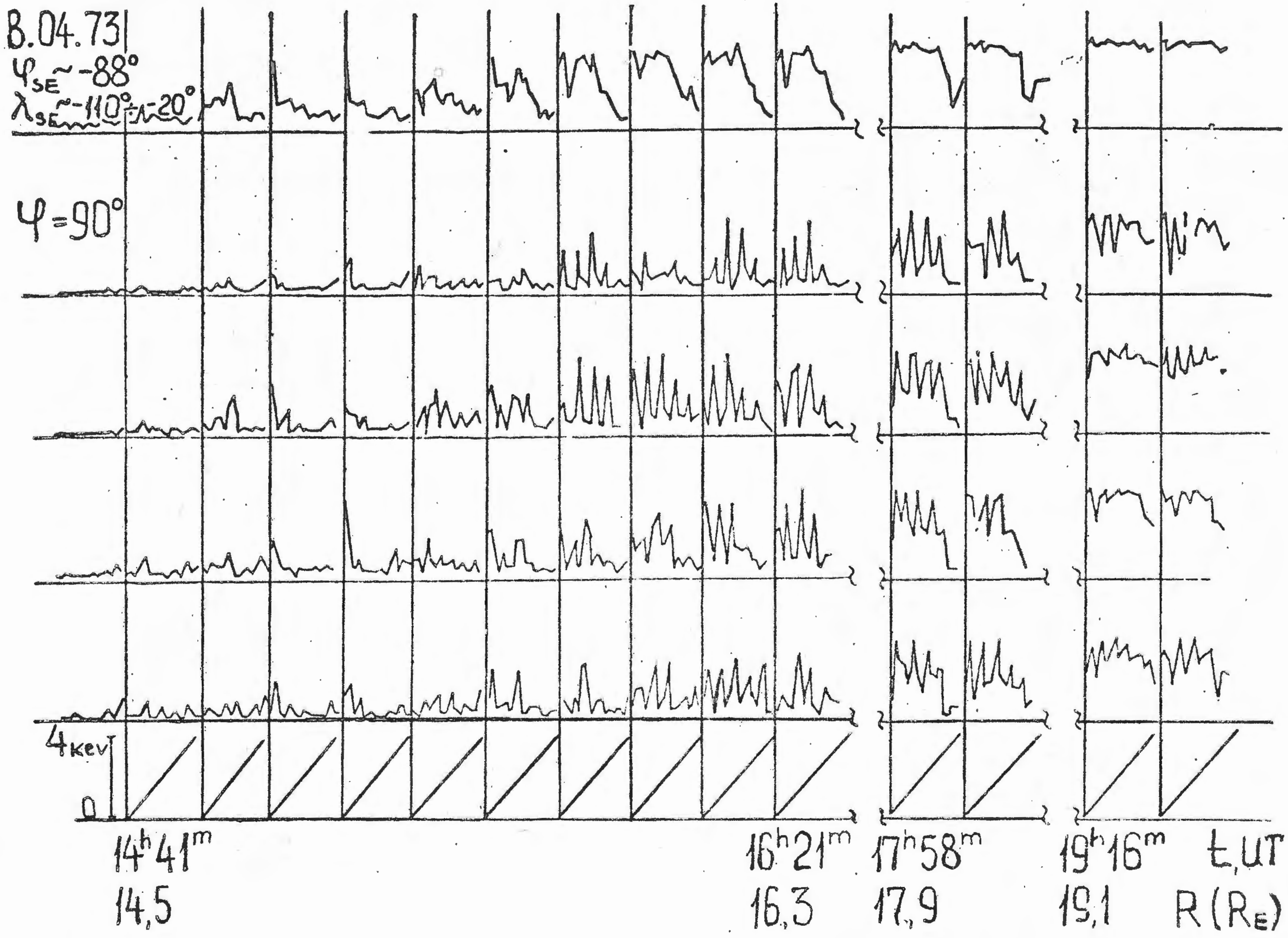

8.04.73
$\varphi_{SE} \sim -88^\circ$
$\lambda_{SE} \sim -110^\circ \div \sim -20^\circ$
$\varphi = 90^\circ$
4 keV
0
$14^h 41^m$
14,5
$16^h 21^m$
16,3
$17^h 58^m$
17,9
$19^h 16^m$
19,1
t, UT
R (R_E)

Fig 7

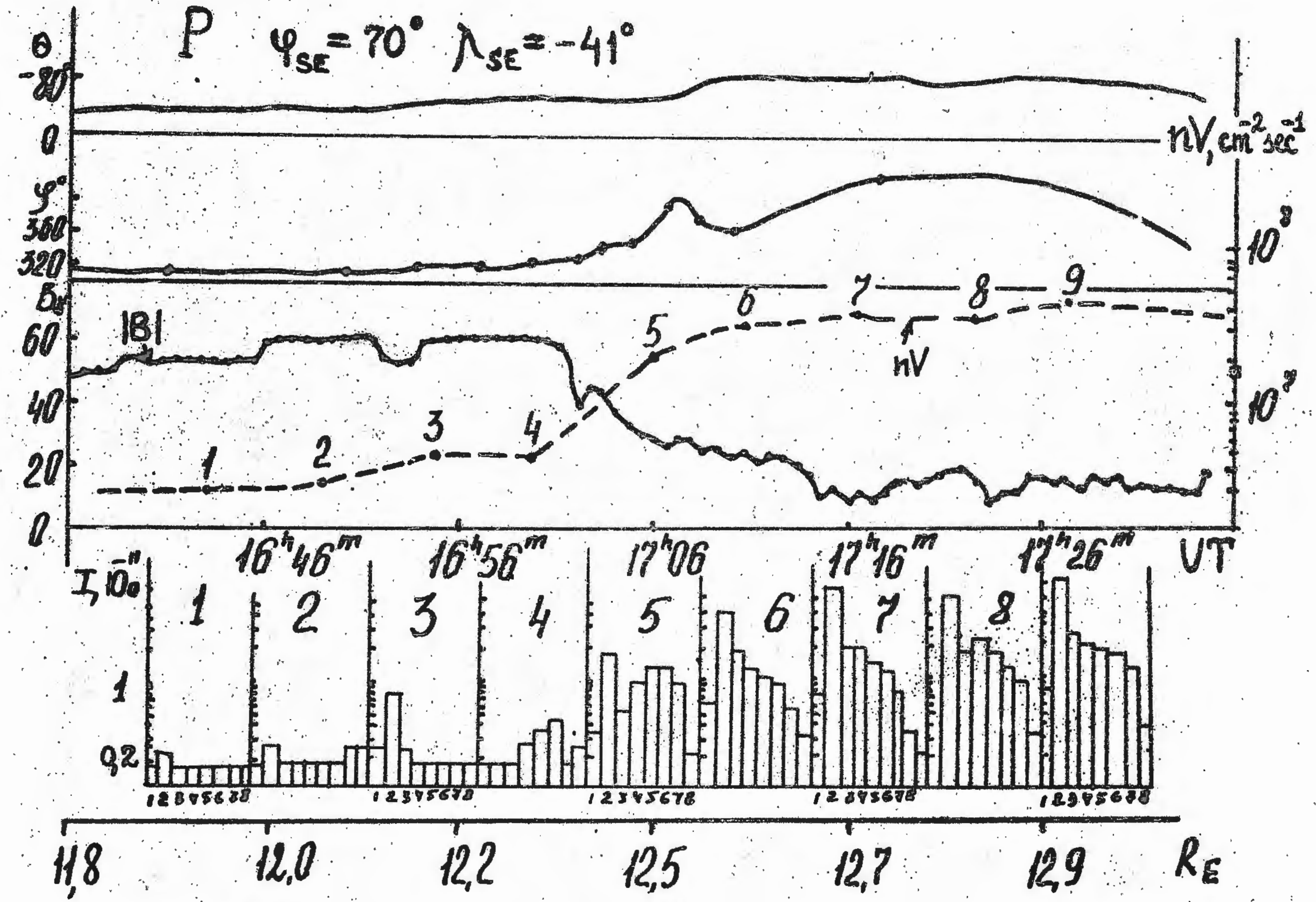

P $\varphi_{SE} = 70°$ $\lambda_{SE} = -41°$
θ
-80
0
φ°
360
320
B_z
60
40
20
0
|B|
$nV, cm^{-2} sec^{-1}$
10^8
10^7
nV
UT
16h46m
16h56m
17h06
17h16m
17h26m
$I, 10^{-11}$
1
0.2
R_E
11,8
12,0
12,2
12,5
12,7
12,9

Fig. 8